

Finite range effects of nuclear force in intermediate energy heavy ion collisions

Lie-Wen Chen^{1,2,3}, Feng-Shou Zhang,^{1,2,4} Wen-Fei Li^{1,2}

¹ *Center of Theoretical Nuclear Physics, National Laboratory of Heavy Ion Accelerator, Lanzhou 730000, China*

² *Institute of Modern Physics, Academia Sinica, P.O. Box 31, Lanzhou 730000, China*

³ *Department of Applied Physics, Shanghai Jiao Tong University, Shanghai 200030, China*

⁴ *CCAST (World Laboratory), P.O. Box 8730, Beijing 100080, China*

Within the framework of an isospin-dependent quantum molecular dynamics model, the zero-range 2-body part of the Skyrme interaction is replaced by a finite-range Gaussian 2-body interaction. From the transverse momentum analysis in the reaction of system $^{93}\text{Nb} + ^{93}\text{Nb}$ at energy of 400 MeV/nucleon and impact parameter $b=3$ fm, it is shown that the finite-range nuclear force enhances the transverse momentum of the reaction system and it can partly replace the momentum dependent part of the nucleon-nucleon interaction.

PACS number(s): 25.70.-z, 25.75.Ld, 21.30.Fe

I. INTRODUCTION

The heavy-ion transport theory is one of important research frontiers in the theoretical nuclear physics in the last decade. Since 1980s, the beam energy has gone up to intermediate and high energy regions and the high temperature and high dense nuclear matter could be formed in the heavy-ion collisions (HIC's), through which one could investigate the nuclear matter properties at extreme conditions. Correspondingly, theoretical nuclear physicists have established some microscopic heavy-ion transport theory, among which the Boltzmann-Uehling-Uhlenbeck (BUU) equation [1], Boltzmann Langevin (BL) equation [2], Quantum Molecular Dynamics (QMD) model [3], Fermionic Molecular Dynamics (FMD) model [4], and Antisymmetric Molecular Dynamics (AMD) model [5], have been used extensively and successfully. Though these models have respective advantages at different aspects, they have a common character, namely, the zero-range Skyrme-like effective interaction being used in all these models. It is well known, however, that the nuclear force is attractive at long range and repulsive at short range. Hence, the finite-range forces may be as more "realistic" than zero-range Skyrme-like forces. With the zero-range forces, some momentum-dependent terms are quadratic or constant leading to unrealistic behavior while those terms vanish with finite-range forces even though relative momenta go high [6]. At usual relative momenta, below $2k_F$, the behavior of zero-range forces are still acceptable but it is always interesting to study the features of HIC's with finite-range nuclear forces [7].

Based on an isospin-dependent QMD model [8–12] which includes the symmetry potential, isospin dependent nucleon-nucleon (N - N) collisions, Coulomb potential for protons, and isospin dependent Pauli blocking effects, the zero-range 2-body Skyrme interaction is replaced by a finite-range Gaussian interaction. As the first investigation of the finite-range effects, we study the collective flow in reaction $^{93}\text{Nb} + ^{93}\text{Nb}$ at energy of 400 MeV/nucleon and impact parameter $b=3$ fm since the finite range of nuclear force represents momentum-dependence of nuclear force in the momentum space [13] and the collective flow is sensitive to the momentum dependent interaction. The calculated results indicate that the finite-range 2-body interaction actually enhances the transverse momentum, which implies that finite-range nuclear force could replace partly the momentum-dependent part of the N - N interaction and therefore by using the finite-range N - N interaction the momentum dependence of the nuclear forces is considered naturally.

II. MODEL AND METHOD

In the QMD model, nucleon i is represented by a Gaussian form of wave function:

$$\Psi_i(\mathbf{r}, t) = \frac{1}{(2\pi L)^{3/4}} e^{-[\mathbf{r}-\mathbf{r}_i(t)]^2/(4L)} e^{i\mathbf{p}_i \cdot \mathbf{r}/\hbar}. \quad (1)$$

Performing Wigner transformation for Eq. (1), one can get the nucleon's Wigner density distribution in phase space:

$$f_i(\mathbf{r}, \mathbf{p}, t) = \frac{1}{\pi\hbar^3} \exp\left[-\frac{(\mathbf{r}-\mathbf{r}_i(t))^2}{2L} - \frac{(\mathbf{p}-\mathbf{p}_i(t))^2 \cdot 2L}{\hbar^2}\right], \quad (2)$$

where the \mathbf{r}_i and \mathbf{p}_i represent the mean position and momentum of the i th nucleon, respectively, the L is the so-called Gaussian wave packet width (here $L=2.0 \text{ fm}^2$). In the QMD model, then the total interaction potential can read

$$U^{tot} = U^{(2)} + U^{(3)}, \quad (3)$$

and the two-body and three-body potentials, $U^{(2)}$ and $U^{(3)}$ can be given, respectively, by

$$U^{(2)} = \sum_{i(\neq j)} U_{ij}^{(2)} = \sum_{i(\neq j)} \int f_i(\mathbf{r}, \mathbf{p}, t) V_{ij}(\mathbf{r}, \mathbf{r}') f_j(\mathbf{r}', \mathbf{p}', t) d\mathbf{r} d\mathbf{p} d\mathbf{r}' d\mathbf{p}', \quad (4)$$

and

$$\begin{aligned} U^{(3)} &= \sum_{i\neq j, i\neq k, j\neq k} U_{ijk}^{(3)} \\ &= \sum_{i\neq j, i\neq k, j\neq k} \int f_i(\mathbf{r}, \mathbf{p}, t) f_j(\mathbf{r}', \mathbf{p}', t) f_k(\mathbf{r}'', \mathbf{p}'', t) V_{ijk}(\mathbf{r}, \mathbf{r}', \mathbf{r}'') d\mathbf{r} d\mathbf{p} d\mathbf{r}' d\mathbf{p}' d\mathbf{r}'' d\mathbf{p}''. \end{aligned} \quad (5)$$

The two-body interaction V_{ij} includes the local two-body Skyrme interaction V_{ij}^{loc} , the Yukawa (surface) interaction V_{ij}^{Yuk} , the symmetry energy part V_{ij}^{sym} , and the Coulomb interaction V_{ij}^{Coul} . Correspondingly, the total two-body potential in the QMD model is as follows,

$$U^{(2)} = U_{(2)}^{loc} + U^{Yuk} + U^{sym} + U^{Coul} = \sum_{i(\neq j)} (U_{ij}^{loc} + U_{ij}^{Yuk} + U_{ij}^{sym} + U_{ij}^{Coul}), \quad (6)$$

for the forms of U^{Yuk} , U^{sym} , and U^{Coul} , one is referred to Refs. [8,9,14–16]. Refs. [14–16] give a detailed description for the Isospin-QMD (IQMD) model. In the present isospin-dependent QMD model, however, Pauli blocking of neutron and proton is treated respectively, namely, the Pauli blocking is isospin dependent. The two-body Skyrme interaction is given as following form

$$V_{ij}^{loc} = t_1 \delta(\mathbf{r}_i - \mathbf{r}_j). \quad (7)$$

From Eqs. (4) and (7), one can get the two-body Skyrme potential

$$U_{(2)}^{loc} = \sum_{i(\neq j)} U_{ij}^{(loc)} = \sum_{i(\neq j)} t_1 \frac{1}{4\pi L^{3/2}} \exp\left[-\frac{(\mathbf{r}_i - \mathbf{r}_j)^2}{4L}\right]. \quad (8)$$

Similarly, from the three-body Skyrme interaction

$$V_{ijk}^{(3)} = t_2 \delta(\mathbf{r}_i - \mathbf{r}_j) \delta(\mathbf{r}_i - \mathbf{r}_k), \quad (9)$$

one can get the three-body Skyrme potential

$$\begin{aligned}
U_{(3)}^{loc} &= \sum_{i \neq j, i \neq k, j \neq k} U_{ijk}^{(loc)} \\
&= \sum_{i \neq j, i \neq k, j \neq k} t_2 \frac{1}{3^{3/2} (2\pi L)^3} \exp\left[-\frac{(\mathbf{r}_i - \mathbf{r}_j)^2 + (\mathbf{r}_i - \mathbf{r}_k)^2 + (\mathbf{r}_j - \mathbf{r}_k)^2}{6L}\right].
\end{aligned} \tag{10}$$

If one defines the interaction density,

$$\rho_{int}^i(r_i) = \frac{1}{4\pi L^{3/2}} \sum_{j \neq i} \exp\left[-\frac{(r_i - r_j)^2}{4L}\right], \tag{11}$$

then Eqs. (8) and (10) can be approximately combined into

$$U^{loc} = \alpha \left(\frac{\rho_{int}}{\rho_0}\right) + \beta \left(\frac{\rho_{int}}{\rho_0}\right)^\gamma, \tag{12}$$

where the ρ_0 is the normal nuclear matter density, 0.16 fm^{-3} .

For the momentum dependent interaction V_{ij}^{MDI} , we make use of the real part of the optical potential parametrized in Ref. [17] as follows

$$V_{ij}^{MDI} = \delta \ln^2[\varepsilon(\mathbf{p}_i - \mathbf{p}_i)^2 + 1] \delta(\mathbf{r}_i - \mathbf{r}_j). \tag{13}$$

The parameters of Eqs. (12) and (13) are given in Table I, from which one can see two kinds of equations of state (EOS) are commonly used. One is the so-called hard EOS (H, HM) with an incompressibility of $K=380 \text{ MeV}$, and the other is the soft EOS (S, SM) with an incompressibility of $K=200 \text{ MeV}$ [3]. The M refers to the inclusion of the momentum dependent interaction.

If the 2-body Skyrme interaction, Eq. (7), is replaced by a finite-range Gaussian, i.e.,

$$V_{ij}^{loc} = t_1 \frac{1}{\Delta^3 \pi^{3/2}} \exp\left[-\frac{(\mathbf{r}_i - \mathbf{r}_j)^2}{\Delta^2}\right], \tag{14}$$

where the Δ represents the finite-range parameter of N - N interaction, then one can get the Gaussian 2-body effective potential in the QMD model

$$U_{(2)}^{Gau} = \sum_{i(\neq j)} U_{ij}^{(Gau)} = \sum_{i(\neq j)} t_1 \frac{1}{[4\pi(L + \frac{\Delta^2}{4})]^{3/2}} \exp\left[-\frac{(\mathbf{r}_i - \mathbf{r}_j)^2}{4(L + \frac{\Delta^2}{4})}\right]. \tag{15}$$

By comparing Eq. (15) with Eq. (8), one can find that the Gaussian 2-body effective potential can be reached only through replacing the L by $L + \frac{\Delta^2}{4}$ in the 2-body Skyrme potential, namely, Eq. (8). For the zero-range Skyrme two-body interaction, Eq. (7), the short range repulsive core is not considered. Physically, the Eq. (14) is equivalent to simulate the short range repulsive core and therefore Δ should have the same order as radius of the repulsive core, namely, $\Delta \approx 0.4 \sim 0.6 \text{ fm}$. The long range attractive part of the 2-body N - N interaction mainly comes from the Yukawa interaction. In order to observe the effects of Δ on nuclear force, we display in Fig. 1 the finite-range Gaussian 2-body force as a function of the distance between the two nucleons for $\Delta = 0.0, 0.3, 0.5$ and 0.7 fm . Here we set $t_1 = 356 \text{ MeV} \cdot \text{fm}^3$ and it should be noticed that the case of $\Delta = 0.0$ corresponds exactly to the case of zero-range Skyrme two-body force since Eq. (7) is the limitation of Eq. (14) as $\Delta \rightarrow 0$. It is indicated in Fig. 1 that the 2-body nuclear force is attractive and becomes weak gradually with increment of Δ , which imply the finite-range enhances the repulsive effect of nuclear force. This phenomenon is easy to understand since the finite range of nuclear force means momentum-dependence of nuclear force in the momentum space.

Similarly, the zero-range 3-body Skyrme interaction, Eq. (9), can be replaced by finite-range Gaussian 3-body interaction, i.e.,

$$V_{ijk}^{(3)} = t_2 \left(\frac{1}{\Delta^2 \pi}\right)^3 \exp\left[-\frac{(\mathbf{r}_i - \mathbf{r}_j)^2 + (\mathbf{r}_i - \mathbf{r}_k)^2}{\Delta^2}\right], \tag{16}$$

after tedious algebra, one can get the finite-range Gaussian 3-body effective potential in the QMD model, i.e.,

$$U_{(3)}^{Gau} = \sum_{i \neq j, i \neq k, j \neq k} U_{ijk}^{(Gau)} = \sum_{i \neq j, i \neq k, j \neq k} \frac{t_2}{3^{3/2} [2\pi \sqrt{(L + \frac{\Delta^2}{6})(L + \frac{\Delta^2}{2})}]^3} \times \exp[-\frac{(\Delta^2 + 2L)[(\mathbf{r}_i - \mathbf{r}_j)^2 + (\mathbf{r}_i - \mathbf{r}_k)^2] + 2L(\mathbf{r}_j - \mathbf{r}_k)^2}{12(L + \frac{\Delta^2}{6})(L + \frac{\Delta^2}{2})}]. \quad (17)$$

Obviously, this expression is very complicated and has not the simplicity of Eq. (15). In fact, neglecting the Δ^4 and its higher order terms, Eq. (17) can be also simplified as following form,

$$U_{(3)}^{Gau} = \sum_{i \neq j, i \neq k, j \neq k} U_{ijk}^{(Gau)} = \sum_{i \neq j, i \neq k, j \neq k} \frac{t_2}{3^{3/2} [2\pi(L + \frac{\Delta^2}{3})]^3} \times \exp[-\frac{(\mathbf{r}_i - \mathbf{r}_j)^2 + (\mathbf{r}_i - \mathbf{r}_k)^2 + (\mathbf{r}_j - \mathbf{r}_k)^2}{6(L + \frac{\Delta^2}{3})}]. \quad (18)$$

Surprisingly, by comparing Eq. (18) with Eq. (10), one can also find that the Gaussian 3-body effective potential can be reached only through replacing simply the L by $L + \frac{\Delta^2}{3}$ in the 3-body Skyrme potential, namely, Eq. (10). Generally, the zero-range 3-body part of Skyrme interaction can be regarded as a good approximation for the 3-body part of N - N effective interaction. Therefore, we only insert the finite-range 2-body part into the QMD code in the present work.

It should be noted that the replacing of the L by $L + \frac{\Delta^2}{4}$ or $L + \frac{\Delta^2}{3}$ is only for the two-body or three-body effective potential in the QMD model and this replacing dose not affect the other components of the QMD model. Therefore, it is not simply to modify the width of the Gaussian wave packet in the QMD model. The change of the two-body or three-body effective potential only comes from the using of the two-body or three-body finite-range Gaussian interaction (Eq. (14) or (16)) in stead of the two-body or three-body zero-range Skyrme interaction (Eq. (7) or (9)). In fact, the present method is very similar with that of using the well-known finite-range Gogny interaction where the finite range is given by the superposition of two Gaussian function with different ranges and spin-isospin mixtures.

III. RESULTS AND DISCUSSIONS

Within the framework of the above modified QMD model, the transverse momentum is calculated for the reaction of $^{93}\text{Nb} + ^{93}\text{Nb}$ at energy of 400 MeV/nucleon and impact parameter $b=3$ fm for five different potential parameter sets, namely, hard EOS (H), soft EOS (S), soft EOS with momentum dependent interaction (SM), soft EOS with $\Delta = 0.1$ (S 0.1), and soft EOS with $\Delta = 0.5$ (S 0.5). Fig. 2 gives the time evolution of transverse momentum per nucleon for the above five cases. From Fig. 2 one can see clearly that at the initial stage of the collisions the transverse momentum is negative for all cases except for the case with SM, which is easy to understand since for the cases of H, S, S 0.1, and S 0.5, at the initial stage of collisions the attractive nuclear mean field is dominant and consequently the transverse momentum is negative. However, for the case of SM, the initial large relative momentum leads to a large repulsive momentum dependent potential which balances the attractive part of nuclear mean field.

With time evolution, the projectile and target begin to collide, compress, and expand, and the positive transverse momentum is generated. It is shown in Fig. 2 that the transverse momenta have saturated after 40 fm/c for all five cases. In the saturated region, one can see that the largest transverse momentum is observed in the case of H and the smallest in the case of S. The transverse momentum in the case of S 0.1 is little larger than that in the case of S. Comparing to the case of S 0.1, the case of S 0.5 has a larger transverse momentum which is still smaller than that in the case of SM by an amount of 8 MeV/c. These features indicate that the potential parameter set of soft EOS with $\Delta = 0.5$ could replace partly that of soft EOS with the momentum dependent interaction, which implies that the finite-range Gaussian two-body nuclear force could replace partly the momentum dependent part of the N - N interaction.

In order to compare the present calculated results with the experimental data, we display in Fig. 3 the rapidity distribution of the transverse momentum for above five potential parameter sets. The big open circles included in Fig. 3 represent the experimental data which are from the Ref. [18]. The small open circles linked by lines represent the calculated results. Fig. 3 (a) shows the calculated results for the case of H, which indicates that the calculated results are in agreement with the experimental data. Fig. 3 (b) corresponds to the case of SM and it is shown that the calculated results are in better agreement with the experimental data. In Fig. 3 (c) the calculated values linked by solid line and dashed line correspond, respectively, to the cases of S and S 0.1, which are not in good agreement with the experimental data. In the case of S 0.5, Fig. 3 (d) indicates that the calculated results are basically in agreement with the experimental data. These features imply that all the calculated results with potential parameter sets H, SM, and S 0.5 are in agreement with the experimental data while those with potential sets S and S 0.1 fail to reproduce the experimental data. Therefore, the finite-range parameter $\Delta = 0.5$ fm is very reasonable to model the finite-range effect of nuclear force.

Fig. 4 displays the time evolution of transverse momentum per nucleon for free nucleons ($A=1$, solid circles in Fig. 4) and light fragments ($A=2\sim 4$, open circles in Fig. 4) for four different cases, namely, Figs. 4 (a), (b), (c), and (d) correspond, respectively, to the cases of H, S, SM, and S 0.5. In this paper, we construct clusters in terms of the so-called coalescence model [19] with coalescence parameters $R_0 = 3.5$ fm and $P_0 = 260$ MeV/c. One should note that the mass dependence of the transverse momentum shown in Fig. 4 demonstrates the well known increase in magnitude for heavier fragments [20–22]. This phenomenon may be because most nucleons are emitted by the hard stochastic collisions and hence the effect of the mean field is largely erased in the nucleon flow. This argument suggests that the flow of composite fragment carries more direct information of the nuclear EOS than the nucleon flow. From Fig. 4 one can also find that the finite-range Gaussian two-body nuclear force enhances the transverse momenta of fragments and could replace partly the momentum dependent part of the N - N interaction.

IV. CONCLUSIONS

A finite-range Gaussian two-body interaction is applied in stead of the zero-range two-body part of the Skyrme interaction in an isospin-dependent QMD model to simulate the transverse momentum in the reaction of system $^{93}\text{Nb} + ^{93}\text{Nb}$ at energy of 400 MeV/nucleon and impact parameter $b=3$ fm. The calculated results show that the finite-range nuclear force enhances the transverse momentum of the reaction system and it can partly replace the momentum dependent part of the N - N interaction. The calculated results with potential parameter set of soft EOS with finite-range parameter $\Delta = 0.5$ are basically in agreement with the experimental data. Meanwhile, it is shown that the transverse momentum of light fragments is greater than that of free nucleon, which agrees with the results of many experiments.

This work is a primary investigation of the finite-range effects of nuclear force and further consideration is worth performing. For example, the two-body forces adopt the finite-range Gogny forces and meanwhile the finite-range three-body force should be included. In addition, it is very interesting to explore the finite-range effects of other physical phenomena.

V. ACKNOWLEDGMENTS

This work was supported by the National Natural Science Foundation of China under Grant NOs. 19875068 and 19847002, the Major State Basic Research Development Program under Contract NO. G2000077407, and the Foundation of the Chinese Academy of Sciences.

- [1] G. F. Bertsch and S. Das Gupta, Phys. Rep. **160**, 189 (1988).
- [2] Y. Abe, S. Ayik, P.-G. Reinhard, and E. Suraud, Phys. Rep. **160**, 189 (1988).
- [3] J. Aichelin, Phys. Rep. **202**, 233 (1991).
- [4] H. Feldmeier, Nucl. Phys. **A515**, 147 (1990).
- [5] A. Ono, H. Horiuchi, T. Maruyama, and A. Ohnishi, Prog. Theor. Phys. **87**, 1185 (1992).
- [6] D. Idier, M. Farine, B. Remaud, and F. Sébille, Ann. Phys. Fr. **19**, 159 (1994).
- [7] F. Sébille, G. Royer, C. Grégoire, B. Remaud, and P. Schuck, Nucl. Phys. **A501**, 137 (1989).
- [8] L. W. Chen, L. X. Ge, X. D. Zhang, and F. S. Zhang, J. Phys. **G 23**, 211 (1997)
- [9] L. W. Chen, F. S. Zhang, and G. M. Jin, Phys. Rev. C **58**, 2283 (1998).
- [10] L. W. Chen, F. S. Zhang, G. M. Jin, and Z. Y. Zhu, Phys. Lett. **B 459**, 21 (1999).
- [11] F. S. Zhang, L. W. Chen, Z. Y. Ming, and Z. Y. Zhu, Phys. Rev. C **60**, 064604 (1999).
- [12] L. W. Chen, F. S. Zhang, and Z. Y. Zhu, Phys. Rev. C **61**, 067601 (2000).
- [13] P. Ring and P. Schuck, *The Nuclear Many-Body Problem*, New York, Springer-Verlag, p. 172 (1980).
- [14] C. Hartnack, Z. X. Li, L. Neise, G. Peilert, A. Rosenhauer, H. Sorge, J. Aichelin, H. Stöcker, and W. Greiner, Nucl. Phys. **A495**, 303c (1989).
- [15] S. A. Bass, C Hartnack, H. Stöcker, and W. Greiner, Phys. Rev. **C51**, 3343 (1995).
- [16] C. Hartnack, R. K. Puri, J. Aichelin, J. Konopka, S. A. Bass, H. Stöcker, W. Greiner, Eur. Phys. J. **A 1**, 151 (1998).
- [17] J. Aichelin, A. Rosenhauer, G. Peilert, H. Stöcker, and W. Greiner, Phys. Rev. Lett. **58**, 1926 (1987).
- [18] H. G. Ritter, K. G. R. Doss, H. A. Gustafsson, H. H. Gutbrod, K. H. Kampert, B. Kolb, H. Löhner, B. Ludewigt, A. M. Poskanzer, A. Warwick, and H. Wieman, Nucl. Phys. **A447**, 3c (1985).
- [19] F. S. Zhang, E. Suraud, Phys. Rev. C **51**, 3201 (1995).
- [20] D. R. Bowman, G. F. Peaslee, R. T. de Souza, N. Carlin, N. K. Gelbke, W. G. Gong, Y. D. Kim, M. A. Lisa, W. G. Lynch, L. Phair, M. B. Tsang, C. Williams, N. Colonna, K. Hanold, M. A. McMahan, G. J. Wozniak, L. G. Moretto, and W. A. Friedman, Phys. Rev. Lett. **67**, 1527 (1991).
- [21] J. Hubele, P. Kreuzt, J. C. Adloff, M. Begemann-Blaich, P. Bouissou, G. Imme, I. Iori, G. J. Kunde, S. Leray, V. Lindenstruth, Z. Liu, U. Lynen, R. J. Meijer, U. Milkau, A. Moroni, W. F. J. Muller, C. Ngo, C. A. Ogilvie, J. Pochodzalla, G. Raciti, G. Rudolf, H. Sann, A. Schuttauf, W. Seidel, L. Stuttge, W. Trautmann, and A. Tucholski, Z. Phys **A 340**, 263 (1991).
- [22] J. Peter, in Inter. Symp. on Heavy Ion Phys. and Its Appli., Lanzhou, China, 8-12 Oct., Singapore, World Scientific Press, 1990, p.191.

TABLE CAPTIONS

Table I The parameter sets of Eqs. (2) and (3). The S and H refer to the soft and hard equations of state, the M refers to the inclusion of momentum dependent interaction, and the K refers to the incompressibility.

	K(MeV)	α (MeV)	β (MeV)	γ (MeV)	δ (MeV)	$\varepsilon(\frac{c^2}{\text{GeV}^2})$
S	200	-356	303	1.17	—	—
SM	200	-390	320	1.14	1.57	500
H	380	-124	71	2.00	—	—
HM	380	-130	59	2.09	1.57	500

FIGURE CAPTIONS

FIG. 1 The finite-range Gaussian 2-body nuclear force as a function of the distance between the two nucleons for $\Delta = 0.0, 0.3, 0.5$ and 0.7 fm.

FIG. 2 Time evolution of transverse momentum per nucleon for five different potential parameter sets, namely, hard EOS (H), soft EOS (S), soft EOS with momentum dependent interaction (SM), soft EOS with $\Delta = 0.1$ (S 0.1), and soft EOS with $\Delta = 0.5$ (S 0.5) for the reaction $^{93}\text{Nb} + ^{93}\text{Nb}$ at energy of 400 MeV/nucleon and impact parameter $b=3$ fm.

FIG. 3 Rapidity distribution of the transverse momentum for five different potential parameter sets, namely, hard EOS (H) (a), soft EOS with momentum dependent interaction (SM) (b), soft EOS (S) and soft EOS with $\Delta = 0.1$ (S 0.1, the small open circles linked by dashed line) (c), and soft EOS with $\Delta = 0.5$ (S 0.5) (d). The larger open circles are the experimental data and the small open circles are the calculated results.

FIG. 4 Time evolution of transverse momentum per nucleon for free nucleons ($A=1$, solid circles) and light fragments ($A=2\sim 4$, open circles) for four different cases, namely, hard EOS (H) (a), soft EOS (S) (b), soft EOS with the momentum dependent interaction (SM) (c), and soft EOS with $\Delta = 0.5$ (S 0.5) (d). The lines included only to guide the eye.

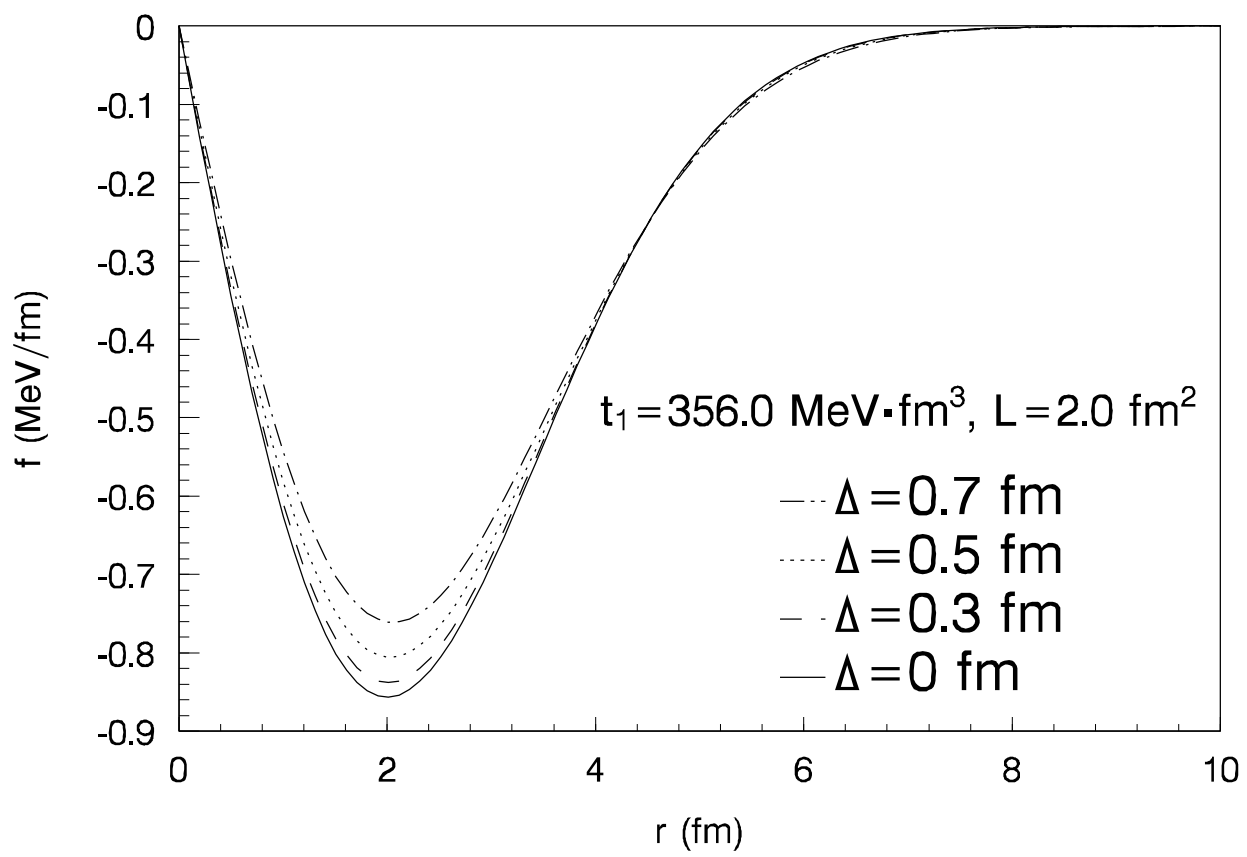


FIG. 1

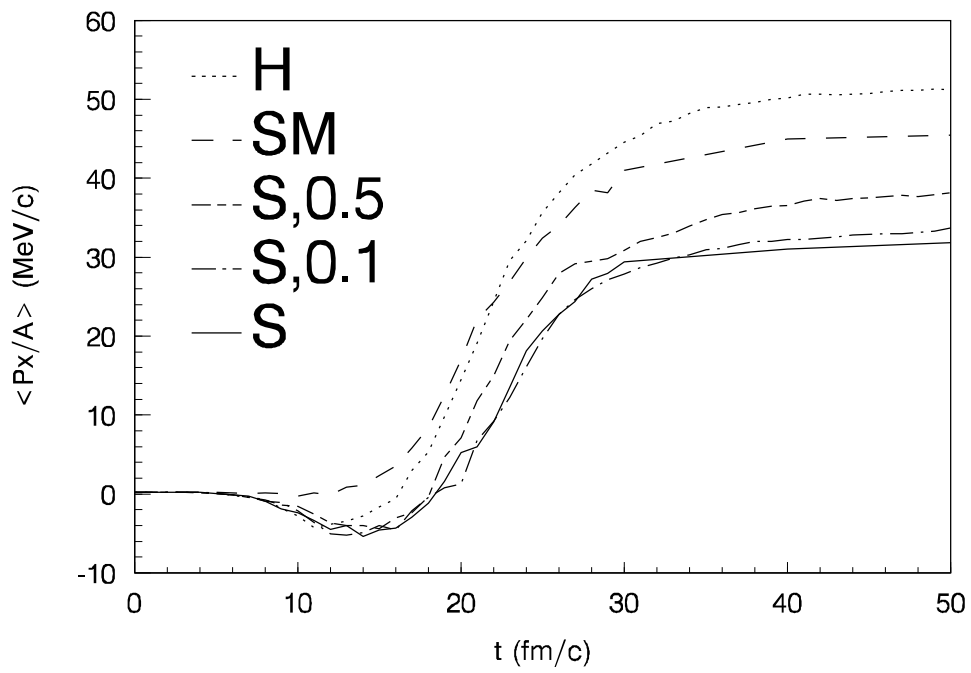


FIG. 2

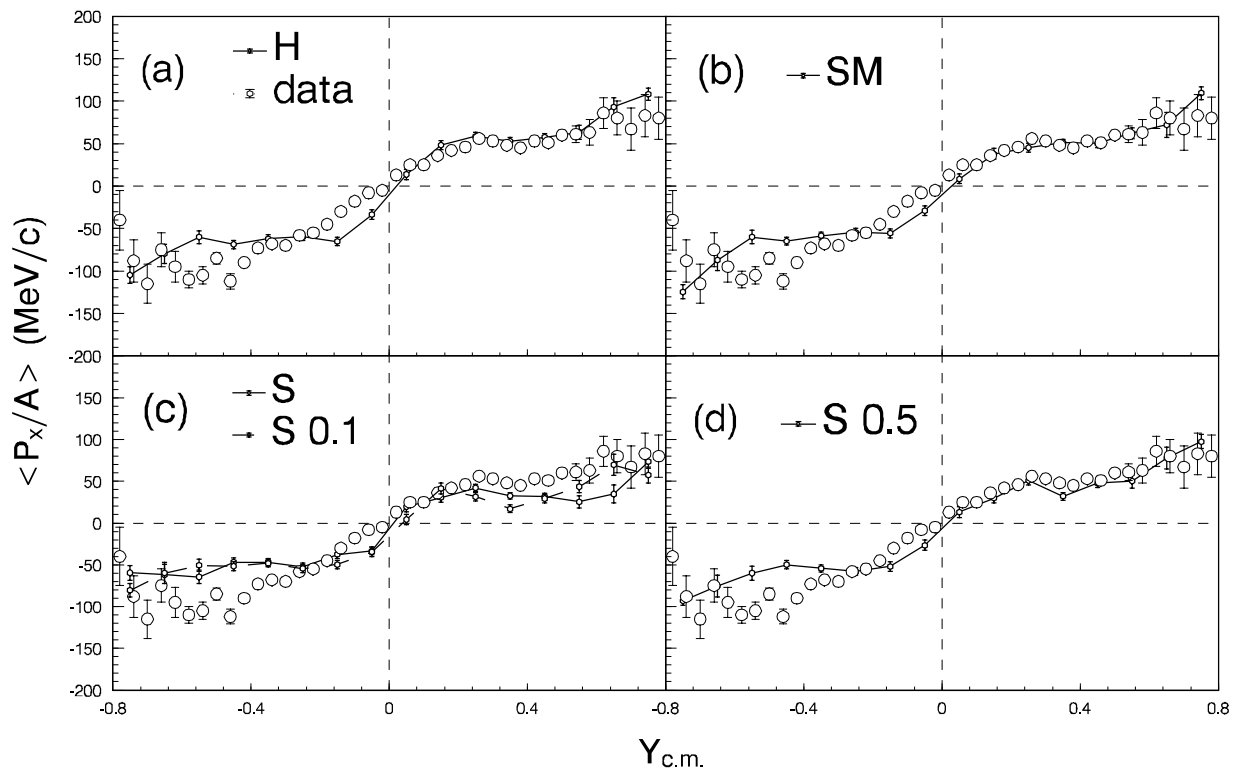


FIG. 3

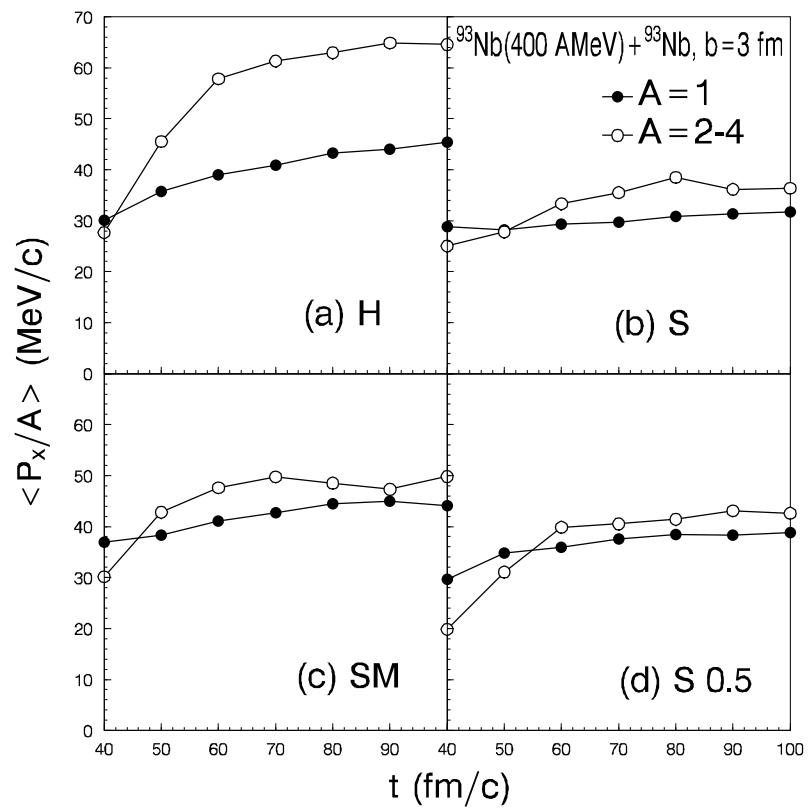


FIG. 4